Electro-assisted assembly of aliphatic thiol, dithiol and dithiocarboxylic acid monolayers on copper

Maho, A.; Denayer, J.; Delhalle, J.; Mekhalif, Z.

Published in:
Electrochimica Acta

DOI:
10.1016/j.electacta.2011.02.020

Publication date:
2011

Document Version
Peer reviewed version

Electro-assisted assembly of aliphatic thiol, dithiol and dithiocarboxylic acid monolayers on copper

A. Maho [a,b], J. Denayer [a,b], J. Delhalle [a], and Z. Mekhalif [a,*]

[a] *Laboratory of Chemistry and Electrochemistry of Surfaces, Facultés Universitaires Notre-Dame de la Paix, Rue de Bruxelles 61, B-5000 Namur, Belgium*

[b] *Fonds pour la Formation à la Recherche dans l'Industrie et dans l'Agriculture, Rue d'Egmont 5, B-1000 Bruxelles, Belgium*

Abstract

Molecular assemblies of organothiol molecules on polycrystalline copper surfaces are a well known process to confer them specific organizational and protective properties. In this paper, an original and promising approach is considered through an electro-assisted adsorption process via a cathodic polarization of the copper substrate. Spectroscopic characterizations (PM-IRRAS, XPS) and electrochemical studies (CV, LSV, cathodic desorption, SECM) highlight and confirm the benefits brought by this methodology in terms of resulting SAMs features and considerable savings of preparation time. In addition to normal alkylthiols with a monopod anchoring group, alkyldithiocarboxylic acid and alkyldithiol monolayers – both bipodal – are characterized with the prospect of forming either easier to remove or more adherent films, respectively.

Key words

Electro-assisted assembly; Alkanethiol; 2-Monoalkylpropane-1,3-dithiol; Dithiocarboxylic acid; Copper

Corresponding author

* Prof. Zineb Mekhalif

Laboratory of Chemistry and Electrochemistry of Surfaces

University of Namur

Rue de Bruxelles, 61, B-5000 Namur – Belgium

Tel : +32 81 72 52 30

e-mail: zineb.mekhalif@fundp.ac.be

1. Introduction

Self-assembled monolayers (SAMs) have been broadly investigated over the past 25 years [1,2]. These organic thin films confer specific features and properties to materials, such as protection against corrosion [3-5], microelectronic devices fabrication [6], lithographic patterning [7,8], thin-film lubrication [9], and molecular recognition [10]. They are well acknowledged for their ease of preparation and great reproducibility to form robust, densely packed and highly ordered films. Those self-assemblies provide and/or control the physical and chemical properties of the resulting surface.

A traditional and widespread model of SAMs consists in a film of organothiol molecules adsorbed on gold [1,2,11]. More recently, growing interests have been devoted to oxidizable metals as substrates in this context [12-15]. In particular, organothiol SAMs have been successfully adsorbed on polycrystalline copper, and the resulting layers act as effective barriers to the penetration of corrosive chemicals to the substrate surface [3,4,16,17]. The oxidation state of copper surface is a key factor for elaborating reproducible and high quality monolayers, as several studies have shown the efficiency of an electrochemical reduction pretreatment of copper to form well defined oriented films with high reproducibility [14,18-20].

The common method of generating organothiol SAMs involves a "*passive*" adsorption mechanism, by simply immersing the substrate into the surfactant solution during a predefined time. Another interesting approach relies on an electro-assisted adsorption mechanism [21-29]. This "*active*" grafting process allows a better assistance and control of the molecular assembly at the surface by involving the interfacial electrical field. This phenomenon could influence several important parameters as molecular orientation, anchoring of reactive head group, and adsorption properties [21,22].

Scores of relating studies carried on gold surfaces have highlighted the major improvement of the structural, organizational and protective properties of organothiol monolayers obtained with a polarized substrate. High quality SAMs have been generated with a significant saving of time with regard to their passive homologues [21-23]. The applied potential has also a fundamental importance, and an optimization of its absolute value has revealed to be critical in certain respects [23,24]. Furthermore, electro-assisted adsorption has provided an easy and fruitful access to mixed monolayers otherwise unreachable by the passive self-assembly methodology [25,26].

Recently, a few works have been devoted to the electro-assisted assembly of organothiols on oxidizable metals and alloys, such as nickel [27], carbon steel [28], and copper [29]. Petrovic *et al.* have lately managed to form *n*-alkanethiol films on polycrystalline copper by electrochemical

potentiodynamic polarization. They point out an increase in the surface packing density, structural order and barrier properties against corrosive environments for those monolayers, in comparison with their self-assembled equivalents [29]. However, there was no information relative to the chemical composition of the interface, as well as for the oxide state of the underlying copper substrate, which has an essential impact on the SAMs properties.

In addition to those aspects, it is also really interesting to investigate the relationship between the nature of the sulfur anchoring group of the organothiol molecules and the stability of the corresponding SAMs. Many studies have focussed on normal alkylthiols (RSH), but other kind of organic surfactants have also attracted some considerable interests. For example, chelating dithiols ($R(SH)_2$) have been recognized to form more stable monolayers, while aliphatic dithiocarboxylic acids (RS_2H) have lead to less stable SAMs which are particularly attractive for applications involving temporary coatings. Relating researches has been pursued as well on gold as on copper substrates [30-34].

The main objective of this work consists in carrying an electro-assisted adsorption of aliphatic thiols, dithiols and dithiocarboxylic acids on copper. Their relative stabilities and properties are studied and compared, while their common and different features with their self-assembled analogues on copper are also discussed. SAMs of *n*-tetradecanethiol (RSH, Fig. 1a), 2-dodecylpropane-1,3-dithiol ($R(SH)_2$, Fig. 1b) and *n*-tetradecanedithiocarboxylic acid (RS_2H, Fig. 1c) are prepared under the same reactive conditions on mechanically polished and electrochemically reduced polycrystalline copper substrates. For the sake of comparison, the three molecules bear a nearly identical alkyl chain.

The quality of the different SAMs is assessed by contact angle goniometry and polarization modulation infrared reflection-absorption spectroscopy (PM-IRRAS), while the binding properties at the interface are investigated by X-ray photoelectron spectroscopy (XPS). The electrochemical stability of the films is checked by cyclic and linear sweep voltammetry, and cathodic desorption. Local electrochemistry characterizations are carried on with scanning electrochemical microscopy (SECM).

2. Experimental

2.1. Materials

The substrates are prepared from pure polycrystalline copper (99.99+%, Goodfellow, CU000749). The 1, 3 and 9 µm diamond pastes used in the polishing process are supplied by Buehler. $HClO_4$, NaOH, NaCl and $LiClO_4$ are purchased from Acros Organic and used as received. Tetrabutylammonium perchlorate (TBAP, Fluka), ferrocene-methanol (FC-MeOH, Aldrich) and KNO_3 (Aldrich) are employed without further purification. N,N-dimethylformamide (lab-scan, HPLC 99.8%), absolute ethanol (Norma pur, Analytical reagent), acetonitrile (lab-scan, HPLC 99.9%) are also used as received, and ultra-pure water (18.2 MΩ cm) is utilized for the aqueous solutions. *n*-tetradecanethiol (RSH, purum, Aldrich), 2-dodecylpropane-1,3-dithiol ($R(SH)_2$, synthesized in the laboratory [32]) and *n*-tetradecanedithiocarboxylic acid (RS_2H, synthesized in the laboratory [32]) are the selected surfactants for the assembling processes.

2.2. Substrate and monolayer preparation

Rectangular-shaped (15 mm x 10 mm) 1 mm thick coupons are cut from polycrystalline copper foils (99.99+%, Goodfellow, CU000749). The samples are mechanically polished on a Buehler-Phoenix 4000 instrument using a silicon carbide paper (P1200) followed by three diamond pastes of different granulometry (9, 3 and 1 µm). The substrates are then treated with UV-ozone for 15 minutes (Jelight 42-220), immersed for 15 minutes in an ethanolic sonication bath, copiously rinsed with absolute ethanol and blown dry in a nitrogen stream. These samples are used as references in several experiments (XPS, electrochemistry), in which they are mentioned as *bare copper* substrates.

For the electro-assisted adsorption process, the copper samples are first electrochemically reduced by applying a potential (E_{red}) of *-1.8 V vs. Ag|AgCl* during 10 minutes in a 5.10^{-2} M TBAP / DMF solution, under nitrogen. Then the potential is shifted to E_{ads} *= -1.2 V vs. Ag|AgCl* to "electro-assist" the adsorption of the organothiol surfactant; at the same time, the surfactant (RSH, $R(SH)_2$ or RS_2H) is introduced in the solution with a 10^{-2} M concentration. This potential remains constant during 10 additional minutes, still under controlled atmosphere. The absolute values of E_{red} and E_{ads} have been determined out of fundamental electrochemical characterizations in 5.10^{-2} M TBAP / DMF solutions of bare and RSH/$R(SH)_2$/RS_2H-covered copper substrates.

Passive self-assemblies are prepared following a parallel protocol [19]. The electrochemical reduction is achieved by applying a potential of -820 mV vs. SCE for 10 minutes in an aqueous solution of $HClO_4$

(0.5 M). Copper coupons are then immediately immersed for 2 hours in a 10^{-2} M organothiol solution (RSH, $R(SH)_2$ or RS_2H) in absolute ethanol.

After reaction, all modified samples (by active and passive process) are immersed for 10 minutes in an ethanolic sonication bath to remove physisorbed molecules and dried under a nitrogen flow.

2.3. SAMs characterization

2.3.1. PM-IRRAS

Polarization modulation infrared reflection absorption spectroscopy (PM-IRRAS) is appropriate for acquiring qualitative information on the nature and the structural organization of films on metal surfaces from the study of the recorded frequencies and their shifts. Spectroscopic data are collected from a Bruker Equinox55 PMA37 equipped with a liquid-nitrogen-cooled mercury-cadmium-telluride (MCT) detector and a zinc-selenide photoelastic modulator. The infrared light reaches the sample surface with an incidence of 85° and is modulated between *s*- and *p*-polarization at a frequency of 50 kHz. Signals generated from each polarization (R_s and R_p) are detected simultaneously by a lock-in amplifier and used to calculate the differential surface reflectivity $\Delta R/R = (R_p-R_s)/(R_p+R_s)$. The spectra are built from a collection of 512 scans at a spectral resolution of 2 cm^{-1}.

2.3.2. XPS measurements

X-ray photoelectron spectroscopy (XPS) is employed to reveal the type of surface chemistry occurring between the copper surface and the organothiol derivative. Spectra are collected on a Surface Science SSX-100 spectrometer. The photoelectrons are excited using an AlK_α radiation as the excitation source (1486.6 eV), collected at 35° from the surface normal and detected with a hemispherical analyzer. The spot size of the XPS source on the sample is about 600 µm, and the analyzer is operated with a pass energy of 20 eV. During data acquisition pressure is kept below (1 x 10^{-9} Torr), and the binding energies of the obtained peaks is made with reference to the binding energy of the C1s line set at 285.0 eV, characteristic of the alkyl moieties. Spectra are fitted using an 80%/20% linear combination of Gaussian and Lorentzian profiles. Peak positions obtained after analysis are found essentially constant (± 0.5 eV).

2.3.3. Contact angle goniometry

Contact angles on the Cu/SAM surface are obtained with a Digidrop Contact Angle Meter (GBX Surface Science Technologies). Measurements are carried out with 3 µl drops of ultra-pure water under ambient atmospheric conditions.

2.3.4. Classical electrochemistry characterization (CV, LSV, cathodic desorption)

Cyclic voltammetry (CV) and polarization curves (LSV) measurements are achieved at room temperature on an EG&G Princeton Applied Research, Potentiostat/Galvanostat Model 263A, in an electrolytic spot-cell (spot Ø: 5.2 mm). The reference and counter electrode consist respectively in a saturated calomel electrode (SCE, +0.246 V vs. SHE) and a platinum foil, the substrate playing the role of the working electrode.

To evaluate the blocking effect of the chemisorbed layers, cyclic voltammetry of bare and modified copper with RSH, $R(SH)_2$ or RS_2H are carried out in aerated 0.1 M NaOH aqueous solution at 20 mV/s from -0.6 to +0.3 V vs. SCE for the forward scan, then from +0.3 to -1.0 V for the backward scan. Oxidation and reduction peaks of copper are well identified in this region [14]. A blocking ratio (*BR*) can be calculated by measuring the area of the copper oxidation peaks for bare copper (charge density of bare copper electrode Q_0) and for modified copper (charge density of modified electrode Q) by applying the formula $BR\ (\%) = 100\times(Q_0 - Q)/Q_0$. This parameter can be used for the quantification of the monolayer coverage on the surface.

Polarization curves are measured on bare and modified substrates in dearated 0.5 M NaCl aqueous solution to determine the corrosion potential E_{cor}, the corrosion current density j_{cor} and the pitting potential E_{pit}. A potential varying from -1.0 to +1.0 V vs. SCE with a scan rate of 5 mV/s is applied.

The cathodic desorption studies are completed on a CH Instruments, Potentiostat Model 440, in an electrolytic spot-cell (spot Ø: 5.2 mm). An Ag/AgCl electrode (+0.210 V vs. SHE) acts as the reference electrode and a platinum foil as the counter electrode, the substrate playing the role of the working electrode. Cathodic desorption of the monolayers is accomplished in a deaerated acetonitrile solution with $LiClO_4$ (0.1 M) using cyclic voltammetry. The working electrode is scanned from -0.5 to -1.7 V vs. Ag/AgCl at 50 mV/s. The experiment is carried out in an acetonitrile solution to prevent the hydrogen evolution reaction which takes place in aqueous solution before the organothiolate electrodesorption [32].

2.3.5. SECM characterization

Scanning electrochemical microscopy experiments are carried out with a CH Instruments, Scanning Electrochemical Microscope Model CHI 900B, employing a three-electrode cell with an Ag/AgCl wire in 3 M KCl as the reference electrode, a platinum wire as the counter electrode, and a commercial CH Instruments 10 µm diameter platinum microdisc ultramicroelectrode (UME) as the working electrode. Copper substrate is not polarized during measurements. A 0.1 M KNO_3 solution is used as supporting electrolyte, and ferrocene–methanol (FC–MeOH) is added with a 1 mM concentration, acting as redox mediator for recording approach curves and imaging.

The copper substrate is fixed to the bottom of the Teflon cell employed. The SECM approach curves are measured with the 10 µm diameter platinum tip. The *RG* ratio between the radius of the insulating sheath r_{glass} and the radius of the active electrode surface r_T is 10. During the tip approach, the UME is polarized to +400 mV vs. Ag/AgCl, while the substrate electrode remains at the open circuit potential (OCP) of the solution. The measurement is carried out by moving the tip stepwise closer to the target surface and recording the current intensity *I* at all tip-surface distances *d*, generating a so-called *approach curve* (a normalized current I/I_0 vs. normalized tip position d/r_T graph). The curve shows an intensive current increase or decrease compared to the initial current value I_0 as the tip-to-target distance is lower than three times the radius of the UME, generating a positive or negative feedback effect, respectively [35,36]. The approach is stopped as sharp change of the current occurs when the tip just touches the substrate surface ($d = 0$). The starting *z*-scan rate during approaching is 10 µm/s. All curves are fitted to the SECM feedback theory assuming process at a conductive (positive feedback) or insulating (negative feedback) substrate.

SECM imaging is carried out by scanning a 300x300 µm area in the feedback mode, with 1mM FC-MeOH as mediator solution. The sample is left at OCP during imaging, while the UME potential is set to +400 mV and the *x,y*-scan rate to 20 µm/s. The tip-to-target distance, kept constant during imaging, is adjusted by amperometric approach: the *z*-approach is usually interrupted when the tip just touches the substrate, then the tip is withdrawn by 5 µm.

3. Results and discussion

3.1. Characterization of aliphatic thiol, dithiol and dithiocarboxylic acid monolayers grafted on copper by electro-assisted adsorption

3.1.1. PM-IRRAS

PM-IRRAS spectroscopy analyses the vibrational characteristics of the monolayers (RSH, $R(SH)_2$ and RS_2H) and brings key data about their structural order, conformation and orientation. Experimental spectra for electro-assisted and passive self-assemblies are presented in Fig. 2a and b, respectively. All reveal four bands in the C-H stretching mode region between 3000 and 2800 cm^{-1}, typical of the asymmetric CH_3 stretching ($\nu_a(CH_3)$) around 2965 cm^{-1}, the asymmetric CH_2 stretching ($\nu_a(CH_2)$) around 2920 cm^{-1}, the symmetric CH_3 stretching ($\nu_s(CH_3)$) around 2877 cm^{-1}, and the symmetric CH_2 stretching ($\nu_s(CH_2)$) around 2850 cm^{-1} [37]. Moreover, Fermi resonance interactions between the lower frequency asymmetric CH_3 deformation mode and the symmetric CH_3 stretching band result in the splitting of the latest, with the apparition of a shoulder on the asymmetric CH_2 stretching signal around 2935 cm^{-1} [12,38].

The absolute positions of methylene stretchings have a significant importance for the assessment of monolayer organization. In the ideal case of solid crystalline $CH_3(CH_2)_{21}SH$ monolayers grafted on gold substrates, the alkyl chains are in a *trans* zig zag conformation, densely packed and highly organized. For these optimal organizational SAMs, values of 2918 and 2850 cm^{-1} are found for $\nu_a(CH_2)$ and $\nu_s(CH_2)$, respectively [38]. When the methylene groups adopt gauche forms and are randomly oriented, those modes are shifted towards higher frequencies which indicates a less ordered film where the alkyl chains are poorly packed [4,12,13,38].

The characteristic wavenumbers measured for $\nu_a(CH_2)$ and $\nu_s(CH_2)$ are reported in Table 1: they first acknowledge the global effective grafting of the three types of SAMs on copper by both active and passive methodologies. The RSH monolayer is densely packed and the alkyl chains are in a *trans* zig zag conformation, as indicated by the wavenumbers of 2920 cm^{-1} for $\nu_a(CH_2)$ and 2850 cm^{-1} for $\nu_s(CH_2)$. Meanwhile, the recorded asymmetric and symmetric CH_2 stretchings frequencies are shifted to higher values (around 2924 and 2852 cm^{-1}) for the two bidentate compounds ($R(SH)_2$ and RS_2H), indicating a conformational disorder of these adlayers. The steric hindrance introduced by the bipodal groups leads to greater interchain spacing, and therefore less opportunity for these alkyl chains to organize and pack via van der Waals interactions. No obvious conformational changes are detected between the $R(SH)_2$ and RS_2H, the frequency shift (+1 cm^{-1}) being too low to be significant.

No significant variations of $\nu_a(CH_2)$ and $\nu_s(CH_2)$ frequency values are observed between active and passive processes for the three types of assemblies. The cathodic polarization of the copper substrate has thus no particular effect on the intrinsic organizational properties of these systems, but leads to the formation of SAMs with similar infrared spectroscopy signatures in shorter times (10 minutes rather than 2 hours).

Nevertheless, an interesting particularity is observed in the case of the electro-adsorbed alkylthiol RSH SAMs. The intensity of asymmetric and symmetric CH_3 stretching vibrations, including the Fermi resonance shoulder at 2935 cm^{-1}, is clearly more pronounced (Fig. 2a). The variation of intensity for those vibration modes leads to the hypothesis that the electro-adsorbed RSH monolayers undergo a modification in the alkyl chain inclination and orientation relative to the substrate surface. Because this tendency is not observed for passively grafted analogous RSH films (Fig. 2b), the difference of orientation seems thus to be a consequence of the electro-assisted adsorption process. Unfortunately, a definite conclusion cannot be extracted from such an analysis due to the roughness and polycrystallinity of the substrates. The change in orientation according the process used (active or passive) seems to take place only for RSH SAMs: no change is noticed for $R(SH)_2$ and RS_2H monolayers (Fig. 2a).

3.1.2. XPS measurements

XPS analysis is essential for acquiring accurate and specific knowledge of the elemental composition of the grafted SAM, and the oxidation state of both sulfur anchoring group and copper substrate. Chemical interactions and relationships occurring at the interface between the RSH, $R(SH)_2$ and RS_2H electro-assembled monolayers and the copper surface can be clearly identified and understood, with regard to other spectroscopic and electrochemical characterizations.

The XPS survey spectra (Fig. 3a) confirm, in comparison with bare copper, the presence of the three monolayers at the interface by showing an increase of the intensity of the carbon peak (C1s) as well as the appearance of characteristic signals for sulfur (S2s and S2p). The efficiency of the electrochemical pre-reduction of copper oxides layer in DMF is also demonstrated by the significant decrease of the oxygen (O1s) signal intensity with respect to bare copper.

The S2p signal (Fig. 3b) highlights the exact nature of the sulfur atoms at the interface. A thiolate Cu-S bond is observed for the three considered SAMs, as indicated by the contribution at 162 eV. No unbound thiols (around 164 eV) or oxidized species like disulfides, sulfinates and sulfonates (around 164, 167 and 169 eV, respectively) are detected. Therefore, no multilayers formation or partial oxidation of the film during formation and/or characterization take place [14,39]. The chemical nature of the anchoring group, and especially the presence of a bipodal group, has no specific effect

on the chemical grafting. Indeed, all sulfur atoms are adsorbed on copper. Intensity ratios of S/Cu, extracted from S2p and Cu2p lines, are reported in Table 2: they indicate a substantial monolayer covering ratio, in a similar range for all cases (S/Cu around 0.1).

Nevertheless, important hydrocarbon contaminations are revealed on the carbon C1s core level. Table 2 lists the CH/S elemental ratios obtained from the contribution of aliphatic chains (285.0 eV) and the S2p line: experimental results are quite high considering the theoretical values. This important carboneous contamination seems to arise from the under potential adsorption process; indeed, when the self-assembly is performed passively, none of the three surfactants leads to high hydrocarbon contaminations. In a previous work, the experimental CH/S ratios obtained for those RSH, $R(SH)_2$ and RS_2H films were significantly lower and reached values of 7.1, 7.0 and 15.3, respectively [32].

This contamination is not limited to hydrocarbonated species: other traces of carbon contaminants like C-O, C=O are also detected with the active methodology. It seems thus that the polarization of the working copper electrode during the assembly process of the films is responsible for simultaneous attraction of contamination species. The absence of nitrogen and chloride signatures on the XPS survey spectra indicates no incorporation of the solvent (DMF) or the electrolytic salt (TBAP). Some degradation of those molecules could take place. Further investigations have still to be pursued to identify the exact nature of the contaminants.

The nature of the underlying copper has then been evaluated. The Cu2p signal cannot be used to distinguish metallic copper from oxidized copper forms. However, the Cu_{LMM} Auger line supplies major information about the nature of copper present at the surface [14]. The efficiency of the electrochemical pretreatment is confirmed (Fig. 3c): on bare copper (without electrochemical reduction), the metal is present on its oxidized forms, as indicated by the line at 570.0 eV, while it is essentially metallic (567.8 eV) after the electro-assisted adsorption of the RSH monolayer. Concerning the bidentate compounds, a partial reoxidation of the substrate during or after the self-assembly process is noticed. Copper is present on both metallic and oxide forms for $R(SH)_2$, while only oxidized copper compounds are detected for RS_2H films.

3.1.3. Contact angle goniometry

Measurements of contact angle on copper surfaces covered with monolayers complete the PM-IRRAS and XPS results by providing worthy information about the composition and the structure of interfaces, and especially the degree of their hydrophobic nature. Water contact angles obtained for SAMs of alkanethiols on gold are characteristic of high quality films and estimated around 112° [40]. Experimental average value of water contact angles measured for RSH monolayers electro-adsorbed

on copper is 104°, while $R(SH)_2$ and RS_2H films both lead to a 103° value. Those results give evidence of hydrophobic surfaces, with the presence of few defects in the films.

3.1.4. Classical electrochemistry characterization

Cyclic voltammetry provides information on the electrochemical stability of electro-adsorbed RSH, $R(SH)_2$ and RS_2H films and their blocking behavior. Recorded voltammograms are shown in Fig. 4, and estimated blocking ratios (*BR*) are reported in Table 3. All results clearly point out the formation of highly stable monolayers with strong insulating features. The RS_2H monolayer is oxidized around +50 mV vs. SCE, while the RSH and $R(SH)_2$ films are stable until +175 mV vs. SCE. Furthermore, blocking ratio is estimated around 82% for RS_2H, and increases up to 97% for RSH and $R(SH)_2$. The electrochemical stability on anodic potentials is thus similar for RSH and $R(SH)_2$, while it decreases for RS_2H monolayers. Their passively self-assembled homologues show a relatively similar trend but present some variations between dithiol and thiol assemblies: $R(SH)_2$ SAMs lead to the highest blocking ratios, thanks to their intrinsic stability [30], followed by RSH and RS_2H assemblies [32].

The stability of the self-assemblies when submitted to cathodic potentials is also evaluated in order to check the resistance to cathodic desorption. Fig. 5 and Table 3 present the obtained curves and desorption potentials values E_{des}. The global behaviors of RSH and $R(SH)_2$ electro-adsorbed monolayers correspond with their passively adsorbed equivalents [32]. By polarizing the copper substrate during the adsorption process, the resulting $R(SH)_2$ film shows an increased cathodic stability comparing to its RSH homologue, with respective experimental E_{des} of -1.39 and -1.23 V vs. Ag/AgCl.

Dithiocarboxylic acid monolayers lead to a very specific behavior: they are characterized by two distinct desorption potentials at -1.05 and -1.32 V vs. Ag/AgCl, while one single peak for both thiol and dithiol equivalents (Fig. 3) is observed. In a first time, the reduction of the double bound (C=S) takes place around -1.05 V vs. Ag/AgCl, and the RS_2H molecule is grafted on the surface only via the thiol function $CH_3(CH_2)_{12}(CS)S^-$ like the classical thiolates. Then, at a potential of -1.32 V vs. Ag/AgCl, the cleavage of this last bond occurs. The corresponding desorption occurs at potentials relatively similar to those found for the RSH and $R(SH)_2$ molecules (Table 3). It is also very interesting to analyze the charge densities of the two desorption peaks: values of 1.3 and 0.1 mC/cm² are respectively measured for the first (-1.05 V) and the second (-1.32 V) peak with the electro-adsorbed RS_2H films (Fig. 5). An opposite trend has been observed in a previous study with passively self-assembled RS_2H SAMs, for which the charge density of the second peak was clearly more intense [32].

All these observations have encouraged us to formulate two distinct hypotheses for the grafting mechanism of dithiocarboxylic acid monolayers, either passively or with electro-assistance. The

passive self-assembly would begin with the grafting via the single bond C-SH ($CH_3(CH_2)_{12}$(CS)**SH**), then via the double bond C=S ($CH_3(CH_2)_{12}$(**CS**)SH), despite the fact that this second step would not be favored in terms of steric hindrance. For the active procedure, the application of E_{ads} *= -1.2 V vs. Ag/AgCl* during the electro-assisted assembly would lead to a simultaneous reduction of the C=S double bond, and thus a reinforced grafting via the corresponding anchoring foot.

It is interesting to point out that, according to PM-IRRAS, the structural properties of the SAMs follow the trend RSH > RS_2H > $R(SH)_2$, while another tendency is observed by electrochemical analyses ($R(SH)_2$ > RSH > RS_2H). Nevertheless, the two statements are complementary rather than contradictory: infrared analyses is informative of the organization and orientation of the alkyl chains relative to the substrate surface, while electrochemistry probes the strength of anchoring of the sulfur atom on copper (S-Cu bond) and the resulting monolayer stability.

The degree of protection against corrosion is assessed by polarization curves (Fig. 6). A significant decrease of corrosion current density j_{cor} is observed for all monolayers with respect to bare copper, from 2.6 (bare copper) to 0.5-0.2 µA/cm² (SAMs) (Table 3). The decrease is quiet pronounced for RSH and RS_2H. Evolution of corrosion and pitting potential values E_{cor} and E_{pit} is more scattered (Table 3); it tends to indicate a "mixed-to-anodic" protective effect for all three systems, with corrosion potential E_{cor} being shifted towards anodic potentials. Concerning the $R(SH)_2$ films, the anodic branch current is more marked and the pitting potential E_{pit} increases sharply to +90 mV vs. SCE, while it remains around -150 mV vs. SCE for bare copper and copper modified with RSH and RS_2H. This trend probably indicates that the metal oxidation reaction is more attenuated in the $R(SH)_2$ case; indeed a similar behavior has already been noticed for passively grafted SAMs [31,32].

3.2. SECM characterization and comparison of passive self-assemblies and electro-assisted assemblies of aliphatic thiols on copper

Scanning electrochemical microscopy (SECM) analyses can lead to a very accurate characterization of the intrinsic insulating properties of the grafted SAMs, as well as a global evaluation of their homogeneity characteristics. While classical electrochemistry experiments (CV, LSV, cathodic desorption) can only be used for large-scale assessments, this local microscopy technique is able to provide specific information on a micrometric scale. In this context, SECM constitutes thus an advantageous technique for a precise comparison of passive self-assemblies with their electro-assembled counterparts. In this section, our interest focuses only on *n*-tetradecanethiol (RSH) SAMs formed by active and passive processes. It is also important to state that the FC-MeOH mediator molecules could penetrate a densely packed SAM, but only to a small extent. The redox mediator molecules will thus reach the substrate surface mainly at pinholes or non-covered areas. Therefore,

although some redox processes can occur at the SAM-solution interface, the SECM response will be mostly sensitive to reactions at defects, which enables a qualitative assessment of adlayer features. Very well ordered films are expected to result in suppressed feedback currents, relatively to more defective layers that would present higher feedback currents [20,36,41].

Fig. 7 shows normalized approach curves recorded on bare and modified copper substrates. I/I_0 ratios measured at $d = 0$ on the experimental curves are also reported in Table 4. Key observations relative to the local conductive or insulating properties of the analyzed surfaces are thus obtained. If bare copper rationally exhibits positive feedback behavior (conductive substrate, with I/I_0 of 1.73), RSH-covered samples present clear negative feedback curves ($I/I_0 < 1$). Those monolayers can therefore be considered as insulating films that inhibit the electron transfer all over the surface. Moreover, a considerable improvement is noticed with the electro-adsorbed RSH SAMs. The I/I_0 ratio reaches a value of 0.19 against 0.54 for the self-assembled equivalent. Although the evolution of these ratios only provides qualitative data, global trends can be drawn from those measurements. The cathodic polarization of the copper substrate during the RSH assembling process seems to have beneficial effects on the film structural and insulating properties, an enhancement which adds up to the important time saving already highlighted.

SECM is also used for recording 300x300 µm images of copper samples modified by RSH, passively and with electro-assistance (Fig. 8). Because of the tip size and positioning, pinholes cannot be directly detected by a feedback mode scanning with the present setup of our SECM instrument. Only micron scale inhomogeneities can be observed, but with short amplitude in both cases. Approach curves give thus more reliable information about the local structure of SAMs, because of the much smaller tip-to-target distance.

4. Conclusions and perspectives

This manuscript focuses on an original and promising method for assembling aliphatic thiol, dithiol and dithiocarboxylic acid molecules on polycrystalline copper surfaces. The electro-assisted adsorption process reveals itself very efficient and profitable for obtaining stable films with high adherence, organization and protection features. Moreover, this methodology permits a significant saving of time in comparison with the “passive” self-assembling approach: only 10 minutes are required to obtain monolayers with similar – if not better – spectroscopic characteristics and global electrochemical properties than self-assembled counterparts made up in two hours. PM-IRRAS, contact angle goniometry and XPS studies confirm the efficiency of the SAMs grafting, but also reveal an important hydrocarbon contamination rate at the interface with copper. Classical electrochemistry measurements (CV, LSV, cathodic desorption) point out the high stability of all formed systems, in addition to their good global protective properties. Furthermore, SECM characterizations directly highlight the reinforcement of the insulating comportment of electro-adsorbed alkanethiol films thanks to the substrate cathodic polarization.

Several parameters can be further tested to optimize the global properties of the films: absolute value of the applied adsorption potential, solvent, supporting electrolyte, and temperature are good conceivable examples. In particular, the use of ionic liquids for the passive self-assembling as well as the electro-assisted assembling of organothiols on copper has the potential to open multiple and exciting perspectives.

Acknowledgement

A. Maho and J. Denayer are grateful to FNRS-FRIA for fellowship.

References

[1] A. Ullman, An Introduction to Ultrathin Organic Films from Langmuir-Blodgett to Self-Assembly, Academic press, NY, 1991.

[2] M. Kind, C. Wöll, Prog. Surf. Sci 84 (2009) 230.

[3] G.K. Jennings, P.E. Laibinis, Colloids Surf. A 116 (1996) 105.

[4] G.K. Jennings, J.C. Munro, T.H. Yong, P.E. Laibinis, Langmuir 14 (1998) 6130.

[5] M. Metikos-Hukovic, R. Babic, Z. Petrovic, D. Posavec, J. Electrochem. Soc. 154 (2007) C138.

[6] Z. Huang, P.C. Wang, A.G. MacDiarmid, Y. Xia, G.M. Whitesides, Langmuir 13 (1997) 6480.

[7] A. Kumar, G.M. Whitesides, Science 263 (1994) 60.

[8] C. Zhao, M. Burchardt, T. Brinkhoff, C. Beardsley, M. Simon, G. Wittstock, Langmuir 26 (2010) 8641.

[9] A. Terfort, N. Bowden, G.M. Whitesides, Nature 386 (1997) 162.

[10] N.K. Chaki, K. Vijayamohanan, Biosens. Bioelectron. 17 (2002) 1.

[11] A. Ullman, Chem. Rev. 96 (1996) 1533.

[12] P.E. Laibinis, G.W. Whitesides, D.L. Allara, Y.T. Tao, Y.T. Parikh, R.G. Nuzzo, J. Am. Chem. Soc. 113 (1991) 7152.

[13] H. Ron, H. Cohen, S. Matlis, M. Rappaport, I. Rubinstein, J. Phys. Chem. B 102 (1998) 9861.

[14] Z. Mekhalif, F. Sinapi, F. Laffineur, J. Delhalle, J. Electron Spectrosc. Relat. Phenom. 121 (2001) 149.

[15] Z. Mekhalif, L. Massi, F. Guittard, S. Geribaldi, J. Delhalle, Thin Solid Films 405 (2002) 186.

[16] P.E. Laibinis, G.M. Whitesides, J. Am. Chem. Soc. 114 (1992) 9022.

[17] Y. Yamamoto, H. Nishihara, K. Aramaki, J. Electrochem. Soc. 140 (1993) 436.

[18] Z. Mekhalif, G. Fonder, F. Laffineur, J. Delhalle, J. Electroanal. Chem. 621 (2008) 245.

[19] G. Fonder, F. Laffineur, J. Delhalle, Z. Mekhalif, J. Colloid Interface Sci. 326 (2008) 333.

[20] G. Fonder, C. Volcke, B. Csoka, J. Delhalle, Z. Mekhalif, Electrochim. Acta 55 (2010) 1557.

[21] D.E. Weisshaar, B.D. Lamp, M.D. Porter, J. Am. Chem. Soc. 114 (1992) 5860.

[22] H. Ron, I. Rubinstein, J. Am. Chem. Soc. 120 (1998) 13444.

[23] C.M.A. Brett, S. Kresak, T. Hianik, A.M.O. Brett, Electroanalysis 15 (2003) 557.

[24] Z. Petrovic, M. Metikos-Hukovic, R. Babic, J. Electroanal. Chem. 623 (2008) 54.

[25] F. Ma, R.B. Lennox, Langmuir 16 (2000) 6188.

[26] R. Meunier-Prest, G. Legay, S. Raveau, N. Chiffot, E. Finot, Electrochim. Acta 55 (2010) 2712.

[27] S. Bengio, M. Fonticelli, G. Benitez, A. Hernandez Creus, P. Carro, H. Ascolani, G. Zampieri, B. Blum, R.C. Salvarezza, J. Phys. Chem. B 109 (2005) 23450.

[28] C.R. Weber, L.F.P. Dick, G. Benitez, M.E. Vela, R.C. Salvarezza, Electrochim. Acta 54 (2009) 4817.

[29] Z. Petrovic, M. Metikos-Hukovic, J. Harvey, S. Omanovic, Phys. Chem. Chem. Phys. 12 (2010) 6590.

[30] Y.S. Shon, T.R. Lee, J. Phys. Chem. B 104 (2000) 8192.

[31] J. Denayer, J. Delhalle, Z. Mekhalif, Appl. Surf. Sci. 256 (2009) 1426.

[32] J. Denayer, J. Delhalle, Z. Mekhalif, J. Electroanal. Chem. 637 (2009) 43.

[33] T.C. Lee, D.J. Hounihan, R. Colorado, J.S. Park, T.R. Lee, J. Phys. Chem. B 108 (2004) 2648.

[34] T.R Lee, R. Colorado, WO 02/071151.

[35] A.J. Bard, M.V. Mirkin (Eds.), Scanning Electrochemical Microscopy, Marcel Dekker Inc., N.Y., 2001.

[36] G. Wittstock, M. Burchardt, S.E. Pust, Y. Shen, C. Zhao, Angew. Chem. Int. Ed. 46 (2007) 1584.

[37] D.W. Mayo, F.A. Miller, R.W. Hannah, Course Notes on the Interpretation of Infrared and Raman Spectra, Wiley-Interscience, United States, 2004.

[38] M.D. Porter, T.B. Bright, D.L. Allara, C.E.D. Chidsey, J. Am. Chem. Soc. 109 (1987) 3559.

[39] D.G. Castner, K. Hinds, D.W. Grainger, Langmuir 12 (1996) 5083.

[40] C.D. Bain, E.B. Troughton, Y.T. Tao, J. Evall, G.M. Whitesides, R.G. Nuzzo, J. Am. Chem. Soc. 111 (1989) 321.

[41] C. Cannes, F. Kanoufi, A.J. Bard, J. Electroanal. Chem. 547 (2003) 83.

Figures caption

Fig. 1 : Molecular structure of: (a) *n*-tetradecanethiol RSH; (b) 2-dodecylpropane-1,3-dithiol $R(SH)_2$; (c) *n*-tetradecanedithiocarboxylic acid RS_2H.

Fig. 2: PM-IRRAS spectra of copper modified by RSH, $R(SH)_2$ and RS_2H (a) via electro-assisted assembly and (b) via passive self-assembly.

Fig. 3a: XPS survey spectra of bare copper and modified by RSH, $R(SH)_2$ and RS_2H.

Fig. 3b: XPS core level of S2p of copper modified by RSH, $R(SH)_2$ and RS_2H.

Fig. 3c: XPS core level of Cu_{LMM} Auger of bare copper and modified by RSH, $R(SH)_2$ and RS_2H.

Fig. 4: Cyclic voltammetry (20 mV/s, NaOH 0.1 M, r.t.) of bare copper and modified by RSH, $R(SH)_2$ and RS_2H.

Fig. 5: Cathodic desorption (50 mV/s, $LiClO_4$ 0.1 M in acetonitrile, r.t.) of copper modified by RSH, $R(SH)_2$ and RS_2H.

Fig. 6: Polarization curves (5 mV/s, NaCl 0.5 M, r.t.) of bare copper and modified by RSH, $R(SH)_2$ and RS_2H.

Fig. 7: Normalized SECM approach curves (10 µm/s, 1 mM FC-MeOH / 0.1 M KNO_3, r.t.) of bare copper and modified by RSH via passive self-assembly and electro-assisted assembly.

Fig. 8: SECM images (20 µm/s, 1 mM FC-MeOH / 0.1 M KNO_3, r.t.) of copper modified by RSH via passive self-assembly and electro-assisted assembly.

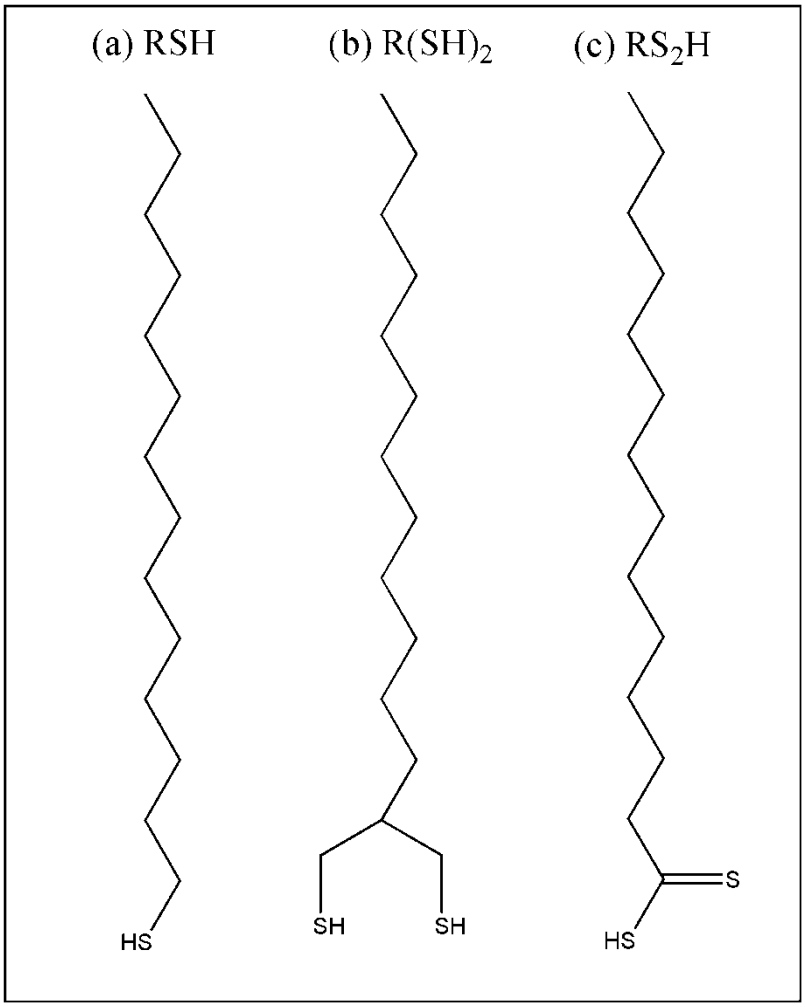

Fig. 1 : Molecular structure of: (a) *n*-tetradecanethiol RSH; (b) 2-dodecylpropane-1,3-dithiol $R(SH)_2$; (c) *n*-tetradecanedithiocarboxylic acid RS_2H.

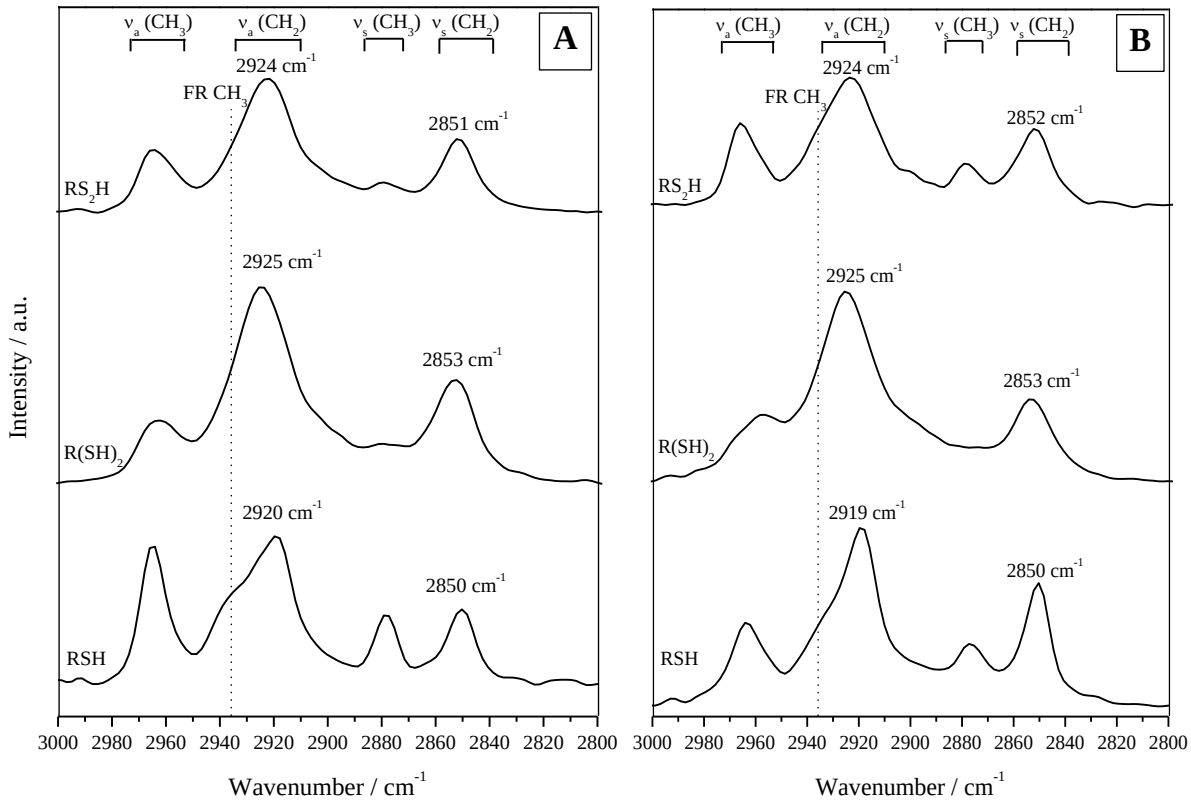

Fig. 2: PM-IRRAS spectra of copper modified by RSH, $R(SH)_2$ and RS_2H (a) via electro-assisted assembly and (b) via passive self-assembly.

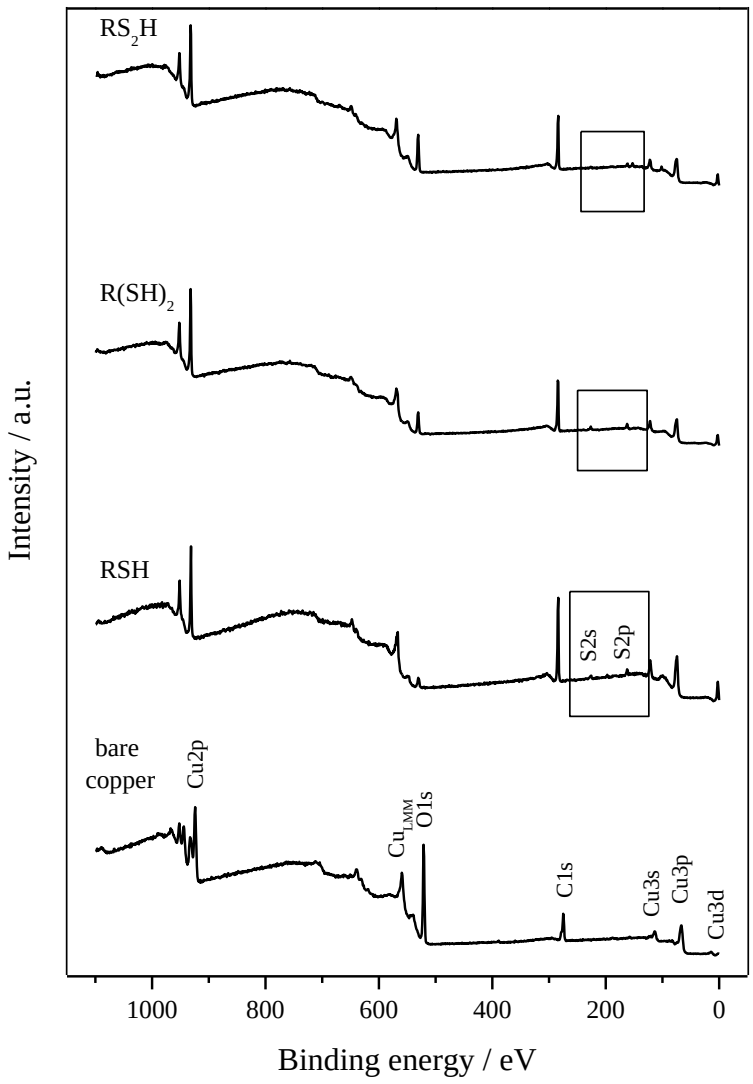

Fig. 3a: XPS survey spectra of bare copper and modified by RSH, $R(SH)_2$ and RS_2H.

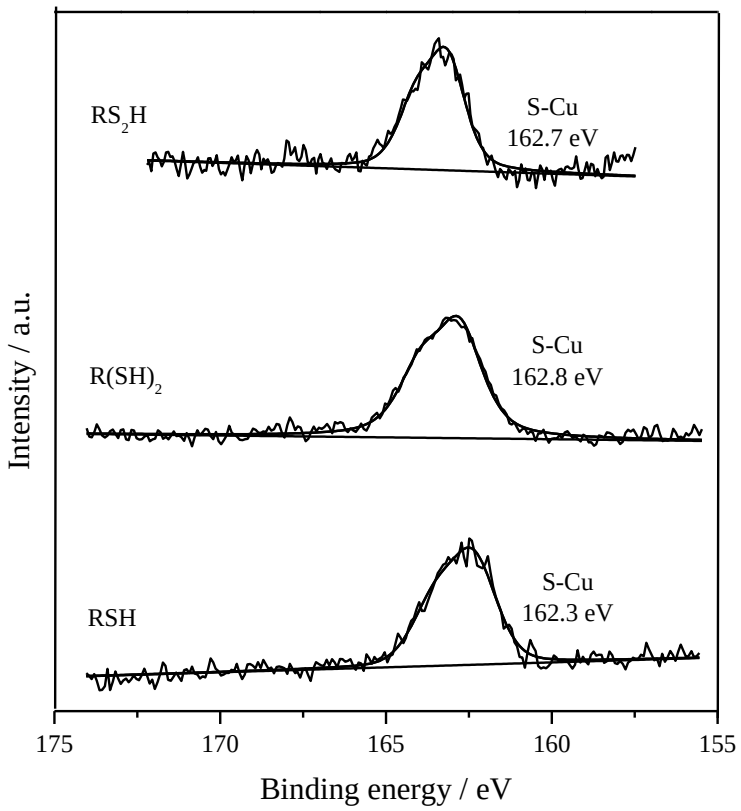

Fig. 3b: XPS core level of S2p of copper modified by RSH, $R(SH)_2$ and RS_2H.

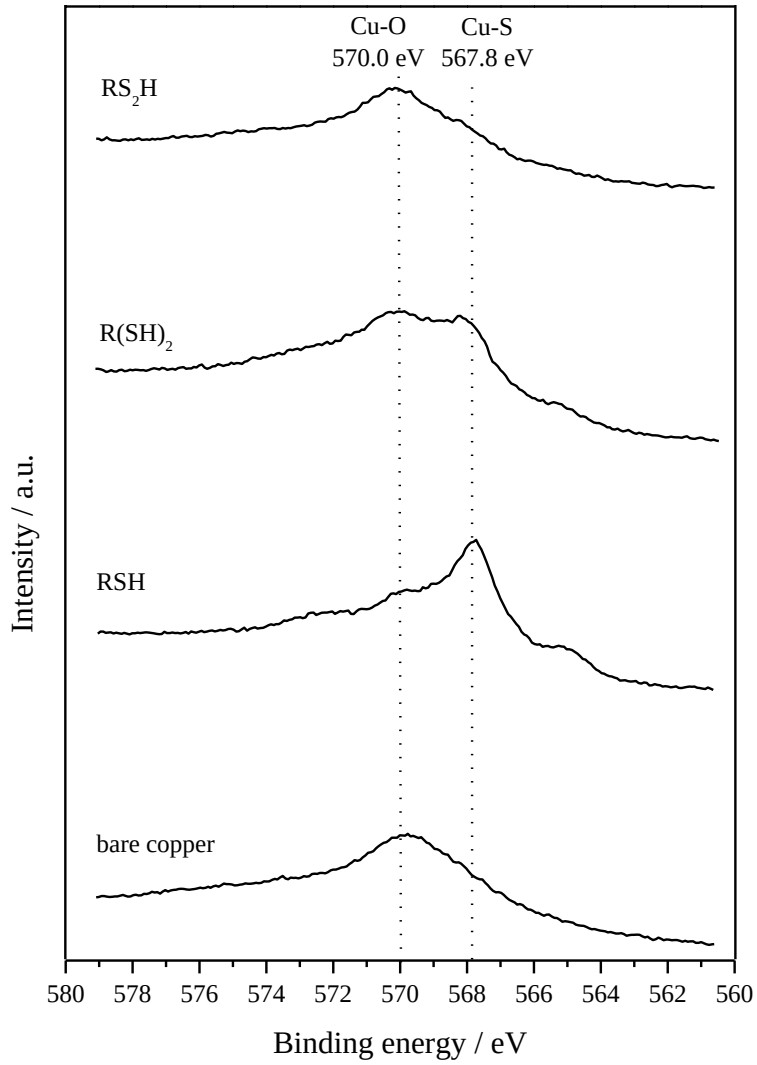

Fig. 3c: XPS core level of Cu_{LMM} Auger of bare copper and modified by RSH, $R(SH)_2$ and RS_2H.

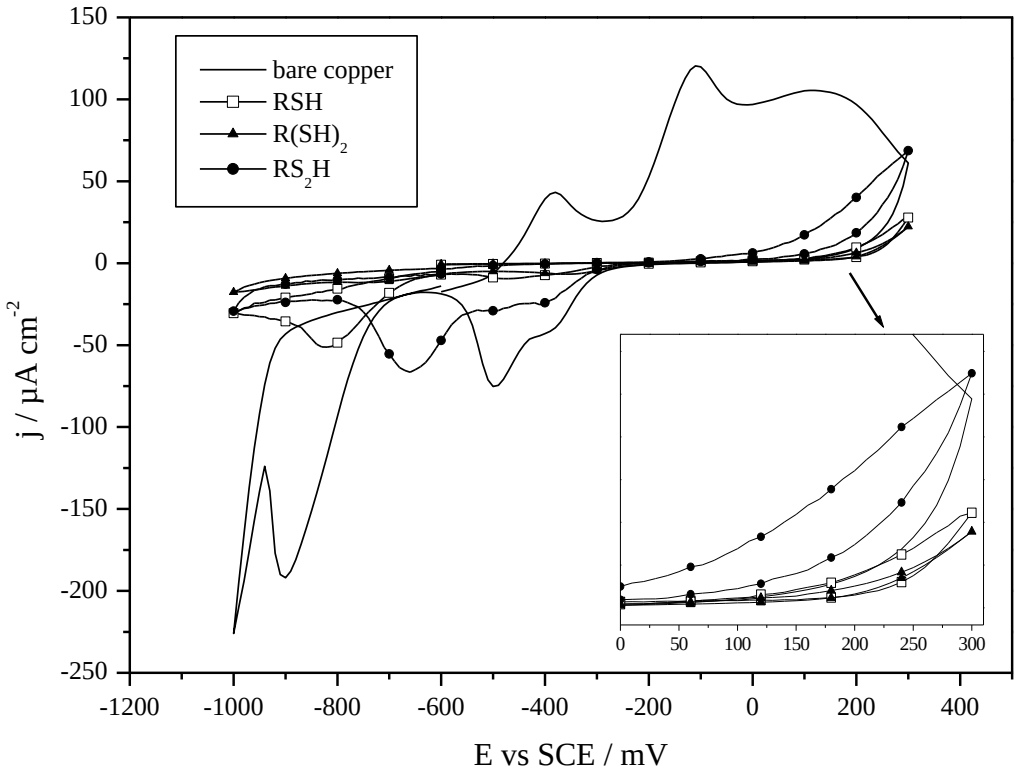

Fig. 4: Cyclic voltammetry (20 mV/s, NaOH 0.1 M, r.t.) of bare copper and modified by RSH, $R(SH)_2$ and RS_2H.

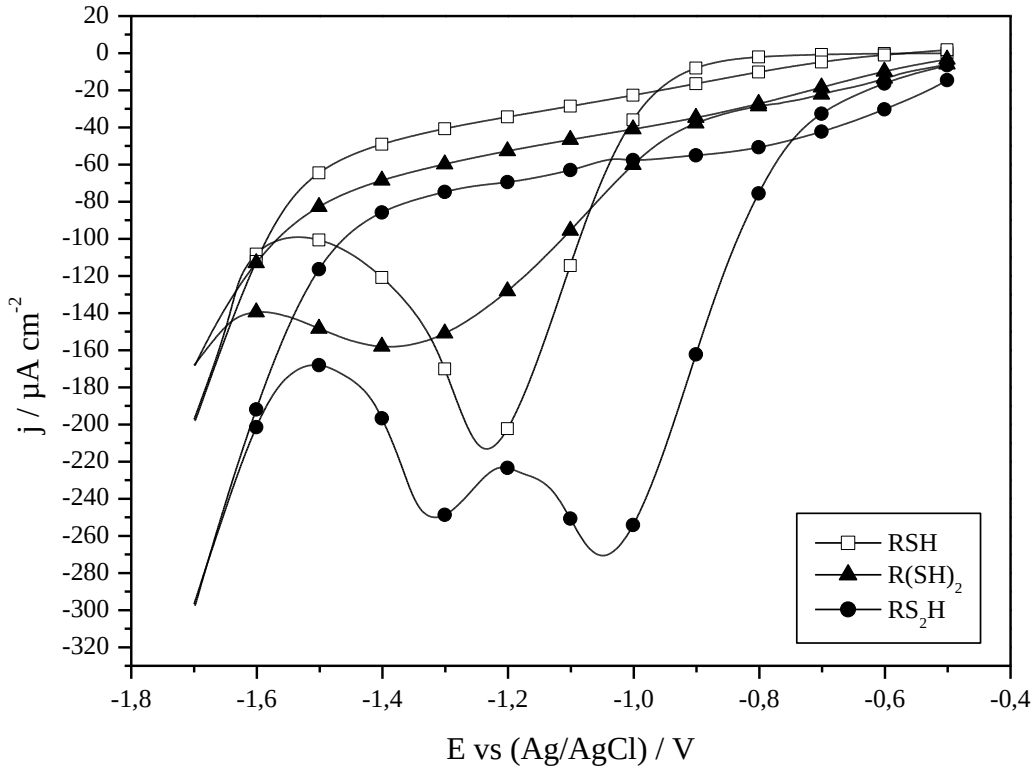

Fig. 5: Cathodic desorption (50 mV/s, $LiClO_4$ 0.1 M in acetonitrile, r.t.) of copper modified by RSH, $R(SH)_2$ and RS_2H.

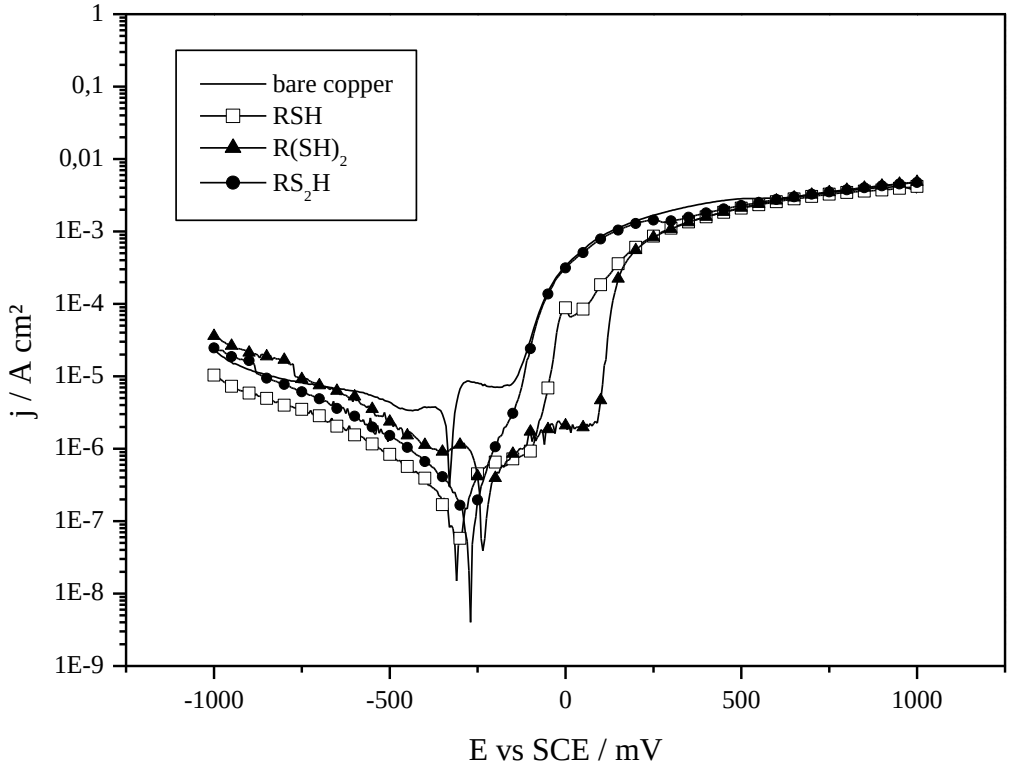

Fig. 6: Polarization curves (5 mV/s, NaCl 0.5 M, r.t.) of bare copper and modified by RSH, $R(SH)_2$ and RS_2H.

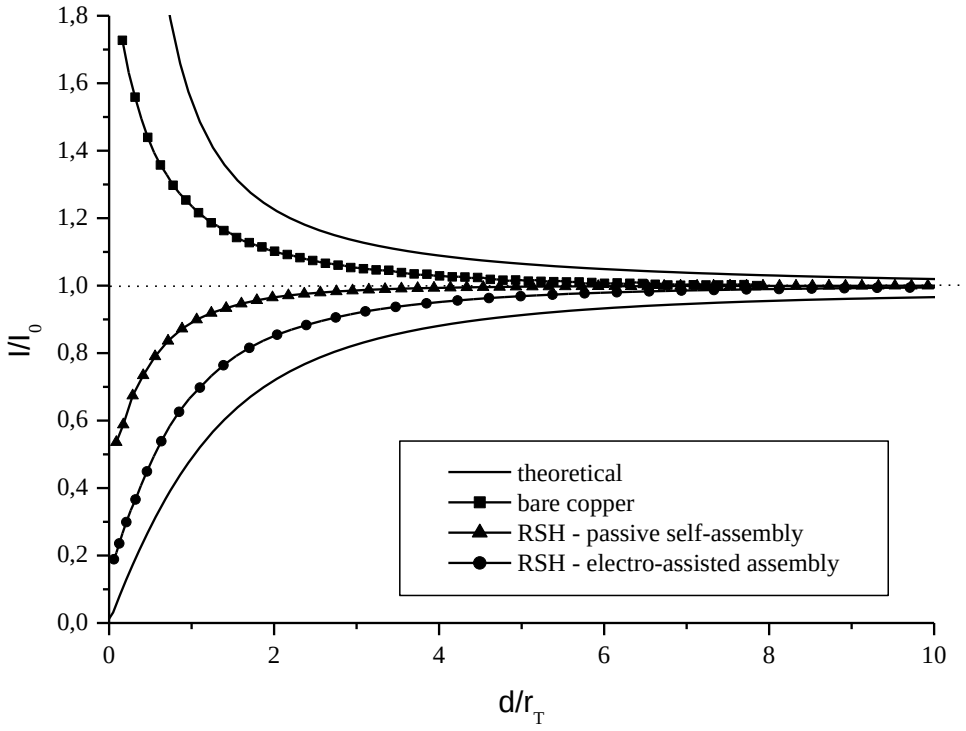

Fig. 7: Normalized SECM approach curves (10 µm/s, 1 mM FC-MeOH / 0.1 M KNO_3, r.t.) of bare copper and modified by RSH via passive self-assembly and electro-assisted assembly.

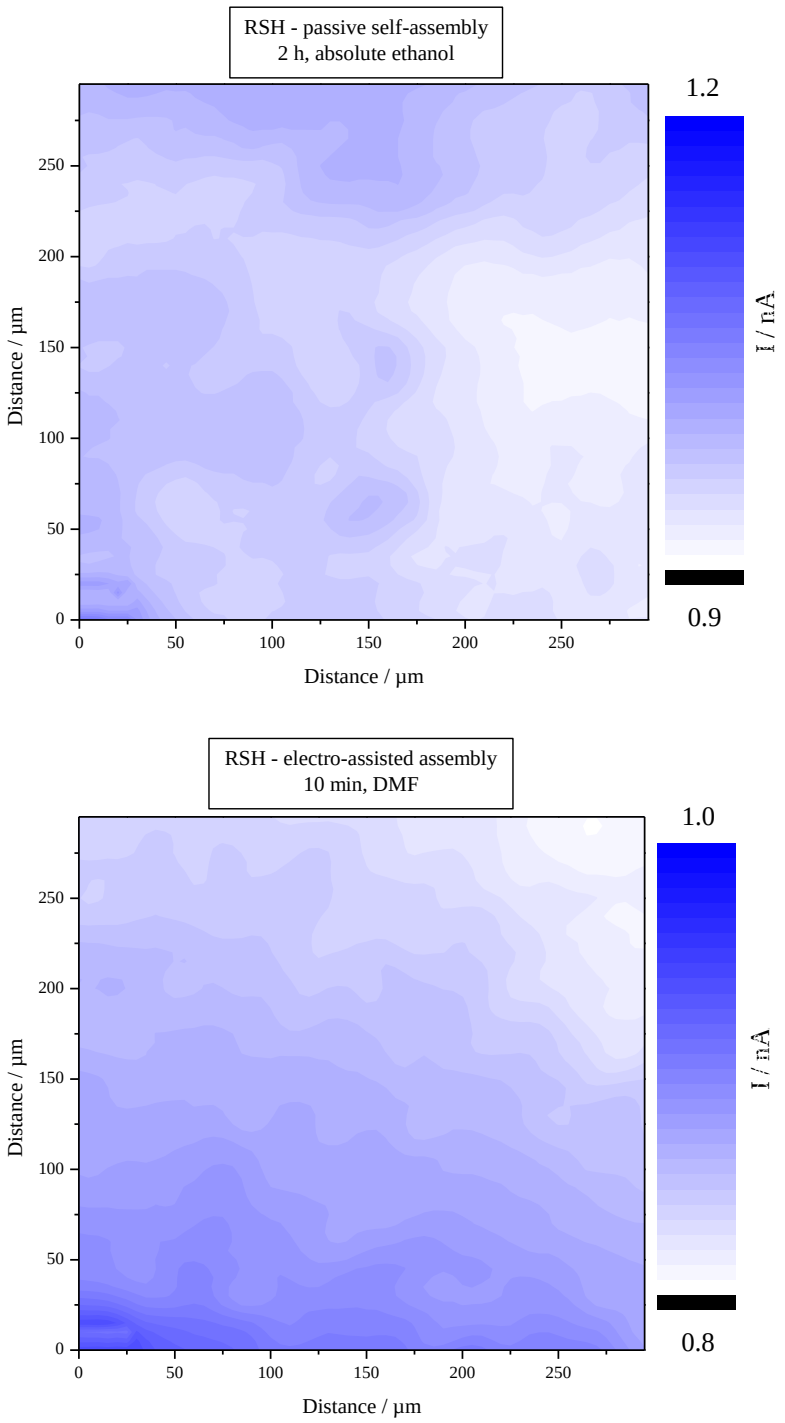

Fig. 8: SECM images (20 µm/s, 1 mM FC-MeOH / 0.1 M KNO_3, r.t.) of copper modified by RSH via passive self-assembly and electro-assisted assembly.

Tables

Table 1: Frequency of CH_2 symmetric and asymmetric stretching for RSH, $R(SH)_2$ and RS_2H for electro-assisted (*active*) and *passive* self-assemblies on copper.

	$\nu_a(CH_2)$ / cm^{-1}		$\nu_s(CH_2)$ / cm^{-1}	
Ideal case	2918		2850	
	Active	***Passive***	***Active***	***Passive***
$R(SH)_2$	2925	2925	2853	2853
RS_2H	2924	2924	2851	2852
RSH	2920	2919	2850	2850

Table 2: S/Cu and CH/S ratios for RSH, $R(SH)_2$ and RS_2H adsorbed on copper. Theoretical values of CH/S ratios are mentioned ( ).

	S/Cu	**CH/S**
RSH	0.11	25.8 (13)
$R(SH)_2$	0.11	18.5 (6.5)
RS_2H	0.07	28.2 (6.5)

Table 3: blocking ratio, desorption potential, corrosion current density, corrosion and pitting potentials of bare copper and modified with RSH, $R(SH)_2$ and RS_2H.

	BR (%)	**E_{des} vs (Ag/AgCl) / V**	**j_{cor} / µA cm^{-2}**	**E_{cor} vs SCE / mV**	**E_{pit} vs SCE / mV**
Bare copper	///	///	2.6	- 329	- 157
RSH	97	- 1.23	0.16	- 310	- 109
$R(SH)_2$	97	- 1.39	0.50	- 221	+ 90
RS_2H	82	- 1.05 / - 1.32	0.18	- 276	- 155

Table 4: I/I_0 values of bare copper and modified by RSH via passive self-assembly and electro-assisted assembly.

	I/I_0
Bare copper	1.73
RSH – passive self-assembly	0.54
RSH – electro-assisted assembly	0.19